



The value of intravoxel incoherent motion diffusion-weighted imaging in predicting the pathologic response to neoadjuvant chemotherapy in locally advanced esophageal squamous cell carcinoma

Tao Song¹ · Qi Yao¹ · Jinrong Qu¹ · Hongkai Zhang¹ · Yan Zhao¹ · Jianjun Qin² · Wen Feng³ · Shouning Zhang¹ · Xianhua Han¹ · Shaoyu Wang⁴ · Xu Yan⁵ · Hailiang Li¹

Received: 2 May 2020 / Revised: 5 July 2020 / Accepted: 31 August 2020 / Published online: 8 September 2020

© European Society of Radiology 2020

Abstract

Objective To explore the value of intravoxel incoherent motion diffusion-weighted imaging (IVIM-DWI) for the prediction of pathologic response to neoadjuvant chemotherapy (NAC) in locally advanced esophageal squamous cell carcinoma (ESCC).

Material and methods Forty patients with locally advanced ESCC who were treated with NAC followed by radical resection were prospectively enrolled from September 2015 to May 2018. MRI and IVIM were performed within 1 week before and 2–3 weeks after NAC, prior to surgery. Parameters including apparent diffusion coefficient (ADC), true diffusion coefficient (D), pseudodiffusion coefficient (D^*), and pseudodiffusion fraction (f) before and after NAC were measured. Pathologic response was evaluated according to the AJCC tumor regression grade (TRG) system. The changes in IVIM values before and after therapy in different TRG groups were assessed. Receiver operating characteristic (ROC) curves analysis was used to determine the best cutoff value for predicting the pathologic response to NAC.

Results Twenty-two patients were identified as TRG 2 (responders), and eighteen as TRG 3 (non-responders) in pathologic evaluation. The ADC, D , and f values increased significantly after NAC. The post-NAC D and ΔD values of responders were significantly higher than those of non-responders. The area under the curve (AUC) was 0.722 for post-NAC D and 0.859 for ΔD in predicting pathologic response. The cutoff values of post-NAC D and ΔD were $1.685 \times 10^{-3} \text{ mm}^2/\text{s}$ and $0.350 \times 10^{-3} \text{ mm}^2/\text{s}$, respectively.

Conclusion IVIM-DWI may be used as an effective functional imaging technique to predict pathologic response to NAC in locally advanced ESCC.

Key Points

- The optimal cutoff values of post-NAC D and ΔD for predicting pathologic response to NAC in locally advanced ESCC were $1.685 \times 10^{-3} \text{ mm}^2/\text{s}$ and $0.350 \times 10^{-3} \text{ mm}^2/\text{s}$, respectively.
- Pathologic response to NAC in locally advanced ESCC was favorable in patients with post-NAC D and ΔD values that were higher than the optimal cutoff values.
- IVIM-DWI can potentially be used to preoperatively predict pathologic response to NAC in esophageal carcinoma. Accurate quantification of the D value derived from IVIM-DWI may eventually translate into an effective and non-invasive marker to predict therapeutic efficacy.

✉ Jinrong Qu
qjryq@126.com

¹ Present address: Department of Radiology, Affiliated Cancer Hospital of Zhengzhou University & Henan Cancer Hospital, 127 Dongming road, Jinshui District, Zhengzhou city, Henan Province, China

² Department of Thoracic Surgery, Affiliated Cancer Hospital of Zhengzhou University & Henan Cancer Hospital, Zhengzhou 450008, China

³ Department of Pathology, Affiliated Cancer Hospital of Zhengzhou University & Henan Cancer Hospital, Zhengzhou 450008, China

⁴ MR Scientific Marketing, Siemens Healthineers, XI'an 710065, China

⁵ MR Scientific Marketing, Siemens Healthineers, Shanghai 201318, China

Keywords Diffusion magnetic resonance imaging · Esophageal neoplasms · Neoadjuvant therapy

Abbreviations

^{18}F -FDG PET/CT	Fluorine-18 fluorodeoxyglucose positron emission tomography-computed tomography
ADC	Apparent diffusion coefficient
CI	Confidence intervals
CT	Computed tomography
D	True diffusion coefficient
D^*	Pseudodiffusion coefficient
DCE-MRI	Dynamic contrast-enhanced magnetic resonance images
DWI	Diffusion-weighted imaging
ESCC	Esophageal squamous cell carcinoma
EUS	Endoscopic ultrasonography
f	Pseudodiffusion fraction
ICC	Intraclass correlation coefficient
iShim	Integrated specific slice dynamic shim
IVIM	Intravoxel incoherent motion
IVIM-DWI	Intravoxel incoherent motion diffusion-weighted imaging
MRI	Magnetic resonance imaging
NAC	Neoadjuvant chemotherapy
NT	Neoadjuvant therapy
RECIST	Response evaluation criteria in solid tumors
ROC	Receiver operating characteristic
ROI	Region of interest
SD	Standard deviation
SNR	Signal-to-noise ratio
TRG	Tumor regression grade
VIBE	Volumetric interpolated breath hold examination

Introduction

Neoadjuvant therapy (NT) has been widely accepted as a standard treatment option for locally advanced esophageal carcinoma [1]. With the development of paclitaxel, neoadjuvant chemotherapy (NAC) has become more widely used in East Asian countries [2]. Many studies have reported that NAC can reduce tumor size, increase surgical resectability, and improve prognosis of patients with esophageal squamous cell carcinoma (ESCC) [2, 3]. However, response to NAC is widely variable [4]. The prognosis of those who do not respond to NAC is worse compared with those who respond, partially due to therapy-induced side effects and delay in surgical resection [5]. Therefore, it is of essential to accurately predict the response of patients with esophageal carcinoma to

NAC. This will help clinicians optimize therapeutic options, by modifying or discontinuing ineffective treatment.

At present, the evaluation of the response to NAC for esophageal carcinoma mainly relies on the measurement of tumor size by traditional modalities such as endoscopic ultrasonography (EUS) and computed tomography (CT), which have shown high accuracy in diagnosis and staging of esophageal carcinoma. However, they are limited in distinguishing between residual tumor, fibrosis, and inflammation [6, 7]. In addition, traditional imaging modalities cannot evaluate the therapeutic efficacy until at least 4 weeks after the end of therapy, and cannot predict early response to NT. Therefore, to date, assessment of response to NT is still unsatisfactory. Fluorine-18 fluorodeoxyglucose positron emission tomography-computed tomography (^{18}F -FDG PET/CT) for response evaluation showed conflicting results and insufficient accuracy, along with the potential of high radiation exposure and increase cost [8, 9]. It is essential to define a safe, non-invasive and effective imaging modality to assess and predict the response to NAC accurately.

Functional MR imaging techniques can reflect biological and microstructural characterization of tumors, so they can quantify therapy-induced changes before anatomic variation in tumor size. Dynamic contrast-enhanced magnetic resonance images (DCE-MRI) can predict early response to chemoradiotherapy in esophageal carcinoma [10, 11]. However, DCE-MRI requires complex pharmacokinetic modelling to calculate the vascular volume fraction of angiogenesis [12]. Diffusion-weighted imaging (DWI) is a functional imaging technique that is widely used in characterizing malignant tumor, monitoring, and predicting therapeutic efficacy [13–16]. However, the DWI-derived apparent diffusion coefficient (ADC) cannot separate diffusion and perfusion information [13].

Intravoxel incoherent motion (IVIM) can differentiate and quantify pure water molecular diffusion and microcirculatory perfusion of the tissue through three parameters calculated by the bi-exponential model: true diffusion coefficient (D), pseudodiffusion coefficient (D^*), and pseudodiffusion fraction (f) [17, 18]. The IVIM technique is increasingly being investigated and has been proven to be more valuable than the ADC value in tumor evaluation and in prediction of therapeutic efficacy of NT [19–25]. However, compared with the conventional DWI sequence, the IVIM sequence requires higher quality imaging and higher signal-to-noise ratio (SNR). To date, research on the application of IVIM sequence in esophageal cancer is still scarce [26].

Although functional MR imaging techniques show powerful capabilities in assessment of tumor microenvironment, histopathological evaluation remains the gold standard. Based on the percentage of viable residual neoplastic cells in relation to

fibrosis/necrosis, tumor regression grade (TRG) can classify tumor pathological response after NT. Compared with tumor size and pathological lymph node status, only TRG can predict disease-free survival in patients with esophageal cancer, and TRG should be considered when evaluating therapeutic efficacy [27]. Because TRG classification requires postoperative pathological specimens, it cannot be used to predict treatment response to NT before treatment.

The primary purpose of our study was to investigate the value of IVIM-DWI sequence for the assessment and prediction of pathologic response to NAC in locally advanced ESCC.

Materials and methods

Study population

This prospective study was approved by the Ethics Committee of our Hospital and all participants signed a written informed consent. Between September 2015 and May 2018, sixty-three consecutive patients pathologically diagnosed with locally advanced ESCC who underwent NAC followed by radical resection were prospectively enrolled.

The inclusion criteria were (1) histological diagnosis of ESCC (stage III); (2) written informed consent; (3) pre-NAC and post-NAC magnetic resonance imaging (MRI) and IVIM sequence (4) without previous history of any malignancy or anticancer treatment; (5) radical surgery for ESCC, with histopathological evaluation.

The exclusion criteria were (1) MRI contraindications; (2) contraindications to NAC; (3) uncompleted NAC; (4) inferior quality of IVIM images (e.g., numerous motion artifacts, low SNR) that would be considered insufficient for further analysis.

Neoadjuvant chemotherapy protocol

All patients underwent two cycles of standard NAC regimen, which consisted of weekly intravenous administration of nedaplatin (50 mg/m²) and paclitaxel (120–150 mg/m²). Radical surgery was performed 3 to 4 weeks (median 23 days) following the completion of NAC.

MRI techniques and imaging analysis

All patients underwent two series of MR scanning within 1 week (median 3 days) before NAC, and 2 to 3 weeks (median 16 days) after completion of NAC, prior to surgery. The IVIM sequence was implemented during the same MR examination. All examinations were performed on a 3-T MR system (MAGNETOM Skyra, Siemens Healthcare) with an anterior 18-element body coil and in-built posterior 32-element spine coil array. All patients were carefully trained for

shallow, slow breath before the examination to reduce respiratory motion artifacts. Raceanisodamine hydrochloride injection (Ningbo Dahongying Pharmaceutical Co.) with a dose of 10 mg was injected intramuscularly 15–20 min before MRI scanning to decrease esophageal peristalsis.

The MRI protocol (detailed parameters in Table 1) consisted of transverse T1-weighted images using volumetric interpolated breath-hold examination (VIBE) sequence, respiratory and electrocardiographically gated T2-weighted fast spin echo with fat suppression. The acquisition times of transverse T1WI and T2WI are 18 s and 3:45 min, respectively. IVIM was acquired using a prototyped integrated specific slice dynamic Shim (iShim) sequence. This sequence first acquires 2D multigradient echo images for each imaging slice with its FOV and orientation adapted from the respective imaging slice. The echo time difference of the first and last echo was chosen such that fat and water alias. Then, a phase difference image was calculated from these two echoes. Nine *b* values from 0 to 800 s/mm² (0, 25, 50, 75, 100, 200, 400, 600, and 800 s/mm²) were applied [28]. The time for the acquisition of the field map was approximately 540 milliseconds per slice. The total acquisition time of IVIM was 3:30 min.

All IVIM images were analyzed independently by two radiologists (T.S. with 15 years and Q.Y. with 6 years of experience in MRI), who were blinded to clinical and pathological outcomes. IVIM raw data was transferred to a work station and processed by MADC software in the FuncTool software package. Region of interest (ROI) of the esophageal lesion was manually delineated on the IVIM-DWI with a *b* value of 400 s/mm² using axial T2-weighted imaging as a reference. The radiologists were instructed to include the entire tumor, except areas of cystic or necrotic degeneration with very high T2 signal. The area of ROI must be greater than 50 mm². ROI of the tumor was automatically transferred to each pseudo color map of IVIM parameters. The values of ADC, *D*, *D*^{*}, and *f* were automatically calculated using MADC software. The changes in IVIM parameters (Δ parameter) before and after NAC were calculated as Δ parameter = post-NAC parameter – pre-NAC parameter.

Response evaluation

An experienced pathologist with 14 years of experience in tumor pathology diagnosis, who was blinded to the IVIM-DWI data, evaluated the pathologic response according to the AJCC (7th edition)—tumor regression grade (TRG) system. The diagnostic criteria were as follows: TRG 3 (poor response), minimal or no tumor kill, extensive residual cancer; TRG 2 (minimal response), residual cancer remaining, but with predominant fibrosis; TRG 1 (moderate response), only small clusters or single cancer cells; TRG 0 (complete response), no remaining viable cancer cells.

Table 1 MRI standard protocol

Parameters	T1-weighted axial	T2-weighted axial	IVIM ($b = 0, 25, 50, 75, 100, 200, 400, 600, 800$ s/mm ²)
TR (ms)	2.72	3000	3200
TE (ms)	0.95	96	56
Slice thickness (mm)	5.0	5.0	5.0
Slice gap (mm)	0.5	0.5	0.5
NEX	1	2	1 ($b = 0-200$); 2 ($b = 400-600$); 3 ($b = 800$)
FOV (mm ²)	360 × 360	380 × 380	340 × 340
Matrix	224 × 384	224 × 384	128 × 128

TR repetition time, TE echo time, NEX number of excitations, FOV field of view

Statistical analysis

All statistical analyses were performed using SPSS version 22.0. Kolmogorov-Smirnov was performed to test whether the measurement data conform to the normal distribution. Continuous variables are presented as mean ± standard deviation (SD). Measurement data that do not conform to the normal distribution are represented as the median (upper and lower quartile). Categorical data are presented as frequencies and percentages.

Comparisons of continuous and categorical clinicopathological factors were processed by *t* test and chi-square test, respectively. The inter-observer consensus in measuring ADC, *D*, *D*^{*}, and *f* was evaluated using the intraclass correlation coefficient (ICC) with 95% confidence interval (CI). The criteria are as follows: 0.00–0.20, poor correlation; 0.21–0.40, fair correlation; 0.41–0.60, moderate correlation; 0.61–0.80, good correlation; and 0.81–1.00, excellent correlation [29].

Compared Student's *t* test (normal distribution) and Wilcoxon rank sum tests (non-normal distribution) were performed to evaluate the change of ADC, *D*, *D*^{*}, *f* pre- and post-NAC. The differences of IVIM-DWI values (i.e., pre- and post-NAC ADC, *D*, *D*^{*}, *f*, and Δ ADC, Δ *D*, Δ *D*^{*}, Δ *f*) in different TRG classifications were verified by means of *t* test of independent sampler (normal distribution) or Wilcoxon rank sum test (non-normal distribution). Values with statistical differences between different TRG groups were further processed by receiver operating characteristic (ROC) curve analysis to calculate the best cutoff thresholds. Specificity, sensitivity, and the area-under-the-curve were computed. A statistically significant difference was identified when $p < 0.05$.

Result

Study population

A total of sixty-three patients were consecutively included in our study. According to the exclusion criteria, two

patients were excluded due to MRI contraindications; four patients were excluded due to contraindications to NAC; six patients were excluded due to incomplete NAC; eleven patients were excluded due to inferior quality of IVIM images, of which five were excluded before NAC, and six were excluded after NAC. The remaining forty patients were enrolled. Patients had a mean age of 61 ± 8 years (age range 44–74 years), and 31 of them were male. The pathological type was all squamous cell carcinoma. The clinicopathologic characteristics of 40 patients showed in our study are detailed in Table 2.

Comparison of clinicopathologic characteristics according to TRG

Twenty-two patients were identified as TRG2, and eighteen as TRG3 in pathologic evaluation. No patients were classified as TRG 0 or TRG 1. Patients were divided into responders ($n = 22$: TRG 2) and non-responders ($n = 18$: TRG 3) with reference to TRG. Baseline clinicopathological characteristics and their statistical association with TRG were summarized in Table 2. No significant differences in clinicopathologic characteristics were found between responders and non-responders ($p > 0.05$).

Comparison of ADC and IVIM parameters before and after NAC

The inter-observer reproducibility was excellent for pre-NAC parameters (ADC: ICC = 0.898, 95% CI = 0.815–0.945; *D*: ICC = 0.925, 95% CI = 0.864–0.960; *D*^{*}: ICC = 0.918, 95% CI = 0.851–0.956; *f*: ICC = 0.848, 95% CI = 0.732–0.917) and post-NAC parameters (ADC: ICC = 0.843, 95% CI = 0.723–0.914; *D*: ICC = 0.867, 95% CI = 0.762–0.927; *D*^{*}: ICC = 0.822, 95% CI = 0.687–0.901; *f*: ICC = 0.823, 95% CI = 0.690–0.902).

As detailed in Table 3, the value of ADC increased significantly after NAC (1.97 ± 0.50 vs $2.51 \pm 0.49 \times 10^{-3}$ mm²/s, $p < 0.001$), and this trend was consistent in *D* value (1.28

Table 2 Baseline clinicopathologic characteristics and their predictive effects ($n = 40$)

Characteristics	All patients	Responders (TRG 2)	Non-responders (TRG 3)	<i>p</i>
Sex				
Female	9	4	5	0.47
Male	31	18	13	
Age (Mean ± SD)	60.8 ± 8.1	59.0 ± 7.6	63.0 ± 8.3	0.12
Location				
Proximal third	8	5	3	
Middle third	26	14	12	0.88
Distal third	6	3	3	
Differentiation				
High	3	2	1	
Middle	20	11	9	0.91
Low	17	9	8	

Values of continuous variables are presented as means ± standard deviation (SD); TRG tumor regression grade

(1.10, 1.41) vs 1.77 (1.45, 1.92) × 10⁻³ mm²/s, $p < 0.001$) and f value (0.34 ± 0.14 vs 0.40 ± 0.15, $p = 0.038$). The change of D^* value before and after treatment was not statistically significant (29.05 (16.80, 47.28) vs 32.20 (18.33, 50.13) × 10⁻³ mm²/s, $p = 0.536$).

Comparison of ADC, IVIM parameters and Δ parameters between responders and non-responders' groups

The post-NAC D (1.82 ± 0.27 vs 1.52 ± 0.39 × 10⁻³ mm²/s, $p = 0.007$) and ΔD (0.65 (0.35, 0.82) vs 0.25(-0.08, 0.31) × 10⁻³ mm²/s, $p < 0.001$) in responders were significantly higher than those in non-responders. The pre-NAC D values of responders were marginally lower than those in non-responders (1.22 ± 0.22 vs 1.42 ± 0.38 × 10⁻³ mm²/s, $p = 0.058$). ΔADC values in responders were slightly higher than those in non-responders (0.66 ± 0.53 vs 0.39 ± 0.36 × 10⁻³ mm²/s, $p = 0.072$), but the difference was not statistically significant. There was no statistical difference in pre-/post-NAC parameters (ADC, D^* , and f) and Δ parameters (ΔD^* and Δf) between responders and non-responders (Table 4). Typical IVIM images for different pathologic responses are presented in Figs. 1 and 2.

Table 3 Mean values of pre- and post-NAC ADC, D , D^* , and f for the overall population ($n = 40$)

Time	ADC (× 10 ⁻³ mm ² /s)	D (× 10 ⁻³ mm ² /s)	D^* (× 10 ⁻³ mm ² /s)	f (%)
Pre-NAC	1.97 ± 0.50	1.28 (1.10, 1.41)	29.05 (16.80, 47.28)	0.34 ± 0.14
Post-NAC	2.51 ± 0.49	1.77 (1.45, 1.92)	32.20 (18.33, 50.13)	0.40 ± 0.15
t value	-7.153	4.471*	0.618*	-2.153
p value	<0.001	<0.001	0.536	0.038

*Z value; ADC apparent diffusion coefficient

Prediction of pathologic response to NAC in locally advanced ESCC

With an area under curve (AUC) of 0.722, post-NAC D exhibited specificity of 66.7%, and sensitivity of 77.3%, when 1.685 × 10⁻³ mm²/s was used as the cutoff value. With a cutoff value for ΔD above 0.350 × 10⁻³ mm²/s, responders may be detected with a specificity of 83.8% and a sensitivity of 77.3% (AUC = 0.859) (Fig. 3).

Discussion

Our results demonstrated that post-NAC D and ΔD values were significantly higher in responders than in non-responders. According to ROC curve analysis, high post-NAC D and ΔD values may help to predict favorable pathologic response in locally advanced ESCC. Moreover, ΔD showed better performance (AUC = 0.859) than post-NAC D (AUC = 0.722) in predicting pathologic response.

In this study, patients with high post-NAC D (> 1.685 × 10⁻³ mm²/s) and high ΔD values (> 0.350 × 10⁻³ mm²/s) had favorable response to NAC, which could be explained by the principle of IVIM introduced by Le Bihan et al [17, 18]. Compared with conventional DWI, the IVIM-derived D values are calculated using the bi-exponential model and

Table 4 Mean values of pre- and post-NAC parameters, Δ parameters, and their predictive effects ($n = 40$)

Parameters	Responders (TRG 2)	Non-responders (TRG 3)	<i>t</i> value	<i>p</i> value
Pre-NAC ADC ($\times 10^{-3}$ mm ² /s)	1.90 \pm 0.49	2.06 \pm 0.52	-0.958	0.344
Post-NAC ADC ($\times 10^{-3}$ mm ² /s)	2.57 \pm 0.43	2.45 \pm 0.55	0.772	0.445
Δ ADC ($\times 10^{-3}$ mm ² /s)	0.66 \pm 0.53	0.39 \pm 0.36	1.850	0.072
Pre-NAC <i>D</i> ($\times 10^{-3}$ mm ² /s)	1.22 \pm 0.22	1.42 \pm 0.38	-1.982	0.058
Post-NAC <i>D</i> ($\times 10^{-3}$ mm ² /s)	1.82 \pm 0.27	1.52 \pm 0.39	2.830	0.007
ΔD ($\times 10^{-3}$ mm ² /s)	0.65 (0.35, 0.82)	0.25(-0.08, 0.31)	-3.865*	<0.001
Pre-NAC <i>D</i> [*] ($\times 10^{-3}$ mm ² /s)	27.65 (15.30, 40.40)	29.05 (16.80, 47.28)	-1.278*	0.201
Post-NAC <i>D</i> [*] ($\times 10^{-3}$ mm ² /s)	31.45 (19.38, 52.40)	32.3 (14.93, 48.25)	-0.530*	0.596
ΔD [*] ($\times 10^{-3}$ mm ² /s)	6.14 \pm 21.90	-2.20 \pm 25.58	1.111	0.273
Pre-NAC <i>f</i> (%)	0.35 \pm 0.13	0.33 \pm 0.15	0.582	0.564
Post-NAC <i>f</i> (%)	0.40 \pm 0.13	0.40 \pm 0.17	-0.024	0.981
Δf (%)	0.046 \pm 0.20	0.07 \pm 0.13	-0.494	0.624

*Z value; ADC apparent diffusion coefficient; TRG tumor regression grade

reflect the true water molecular diffusion. The increased extracellular spaces due to effective chemotherapy may have caused decrease restriction of diffusion of water molecules, which would then yield higher *D* values than those obtained before NAC. ΔD values have high predictable performance in identifying treatment response in locally advanced ESCC, with sensitivity and specificity of 77.3% and 83.8%, respectively. Compared with other imaging modalities such as FDG-PET/CT and DCE-MRI, the diagnostic performance of ΔD value (AUC = 0.859) is superior to the maximum standardized uptake value (SUV_{max}) (AUC = 0.76), K^{trans} (AUC = 0.741)

and K_{ep} (AUC = 0.796), as reported in prior studies (Table 5) [8, 10]. Similar to our results, a previous study reported that the percentage change in *D* value could be utilized to assess response of ESCC to NT [26]. Unlike the study by Zheng et al [26], TRG was introduced as the criterion to evaluate the efficacy of NAC in the current study, compared with Response Evaluation Criteria in Solid Tumors (RECIST) that was used by Zheng et al TRG is a grade scoring system, based on the percentage of viable residual neoplastic cells with reference to necrosis or fibrosis, which can more accurately assess the response of tumor tissue to chemotherapy drugs

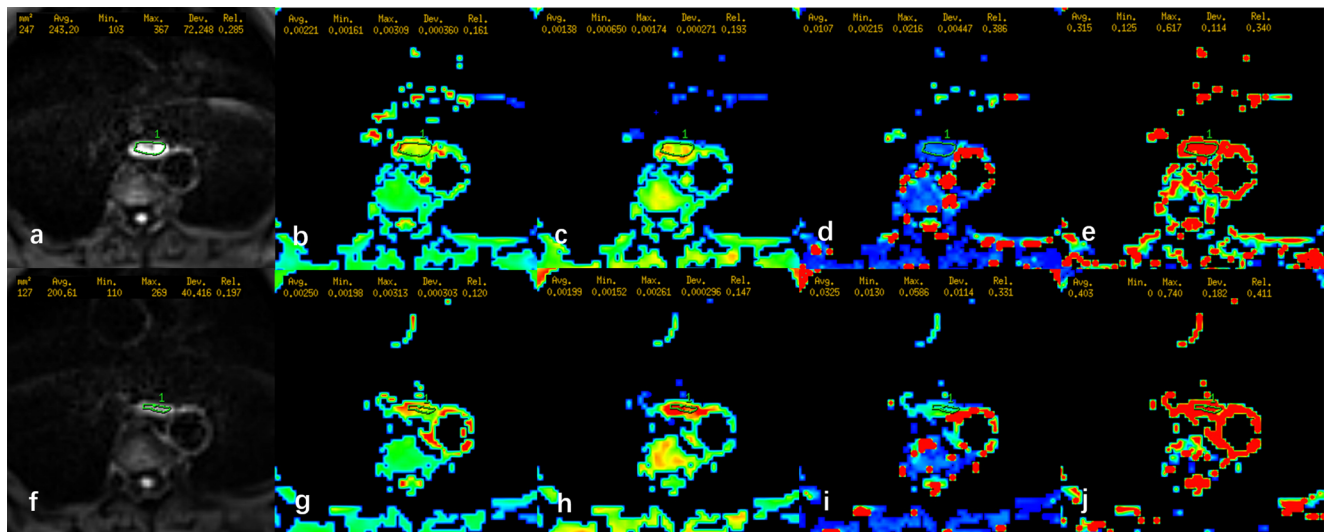


Fig. 1 Typical IVIM pictures of a 68-year-old man with a mid-esophageal squamous cell carcinoma with TRG 2 (responder). **a** Axial diffusion-weighted image ($b = 400$ s/mm²) shows a hyperintense focal esophageal lesion. The ROI (green contours) of tumor was manually delineated on IVIM-DWI. **b–e** The corresponding ADC, *D*, *D*^{*}, and *f* maps show the pre-NAC ADC value of 2.21×10^{-3} mm²/s, a *D* value of 1.38×10^{-3} mm²/s, a *D*^{*} value of 10.7×10^{-3} mm²/s, and an *f* value of

0.32 of the lesion. **f** After NAC, we observed a reduction in tumor size. **g** We observed a rise in the ADC value (post-NAC ADC = 2.50×10^{-3} mm²/s, Δ ADC = 0.29×10^{-3} mm²/s). **h** Post-NAC *D* value was increased to 1.99×10^{-3} mm²/s ($\Delta D = 0.61 \times 10^{-3}$ mm²/s). **i** Post-NAC *D*^{*} value was increased to 32.5×10^{-3} mm²/s ($\Delta D^* = 21.8 \times 10^{-3}$ mm²/s). **j** Post-NAC *f* value was increased to 0.40 ($\Delta f = 0.08$)

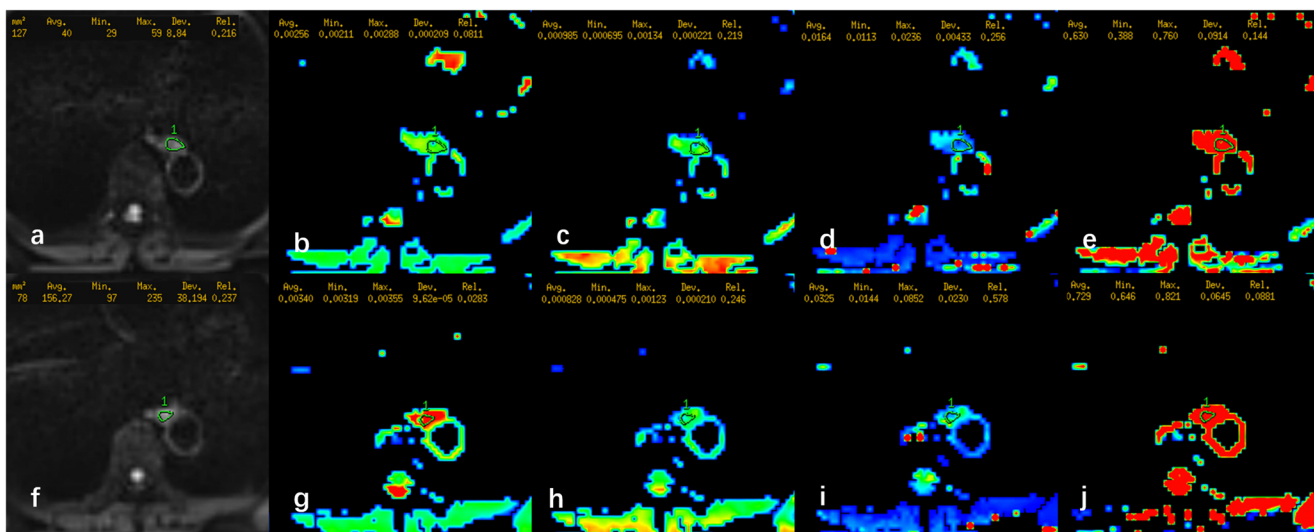


Fig. 2 Typical IVIM pictures of a 60-year-old woman with a mid-esophageal squamous cell carcinoma with TRG 3 (non-responder). **a** Axial diffusion-weighted image ($b = 400 \text{ s/mm}^2$) shows a hyperintense focal esophageal lesion. The ROI (green contours) of tumor was manually delineated on IVIM-DWI. **b–e** The corresponding ADC, D , D^* , and f maps show the pre-NAC ADC value of $2.56 \times 10^{-3} \text{ mm}^2/\text{s}$, a D value of $0.99 \times 10^{-3} \text{ mm}^2/\text{s}$, a D^* value of $16.4 \times 10^{-3} \text{ mm}^2/\text{s}$, and an f value of

0.63 of the lesion. **f** After NAC, we observed a slight reduction in tumor size. **g** We observed a rise in the ADC value (post-NAC ADC = $3.40 \times 10^{-3} \text{ mm}^2/\text{s}$, $\Delta\text{ADC} = 0.84 \times 10^{-3} \text{ mm}^2/\text{s}$). **h** Post-NAC D value decreased slightly to $0.83 \times 10^{-3} \text{ mm}^2/\text{s}$ ($\Delta D = -0.16 \times 10^{-3} \text{ mm}^2/\text{s}$). **i** Post-NAC D^* value increased to $32.5 \times 10^{-3} \text{ mm}^2/\text{s}$ ($\Delta D^* = 16.1 \times 10^{-3} \text{ mm}^2/\text{s}$). **j** Post-NAC f value increased to 0.73 ($\Delta f = 0.10$)

Fig. 3 Analysis of ROC curves, to find an optimal cutoff to distinguish responders from non-responders on the basis of the post-NAC D value and ΔD

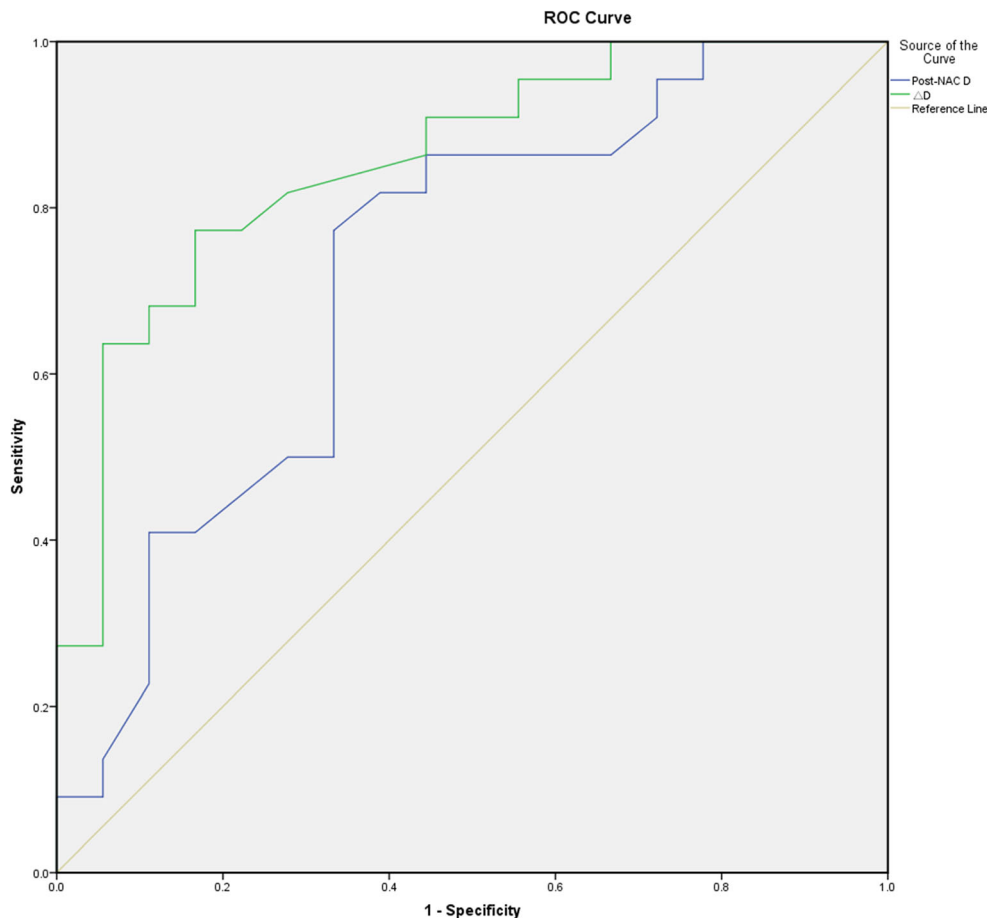


Table 5 Comparison of diagnostic performance between IVIM, DCE-MRI, and PET-CT

Imaging techniques	Parameters	Sensitivity (%)	Specificity (%)	AUC
IVIM	ΔD	77.3	83.8	0.859
DCE-MRI	K_{ep}	77.8	66.7	0.796
	K^{trans}	66.7	66.7	0.741
PET-CT	Post-SUV _{max}	89.7	66.7	0.760

D , true diffusion coefficient; K_{ep} , rate contrast; K^{trans} , volume transfer constant; SUV_{max} , maximum standardized uptake value; AUC , area under curve

compared with RECIST which is based on tumor size changes. TRG has proven to be a reliable prognostic marker for patients with locally advanced esophageal carcinoma [27] and rectal cancer [30]. To our knowledge, our study is the first to apply the IVIM sequence with iShim technique in esophageal cancer. Furthermore, the iShim technique can reduce the geometric deformation and increase the SNR [31, 32], which can improve the accuracy of IVIM parameters fitting effectively and provide excellent inter-observer reproducibility on ADC and IVIM-based parameters. Our finding concerning the D value was consistent with previous studies, which found that an increase in D value can predict chemotherapeutic response in a human gastric cancer mouse model [33] and locally advanced rectal cancer [34].

Previous studies reported that ADC value was useful in assessing and predicting pathologic response to NT in esophageal carcinoma [15, 26, 35, 36]. A prior study with small sample size ($n = 20$) reported that the ΔADC during NT for esophageal cancer seemed highly predictive of histopathologic response, with sensitivity and specificity of up to 82% and 100%, respectively ($AUC = 0.92$). However, the authors acknowledged that the diagnostic performance of ΔADC is likely overestimated to some extent [35]. Two other similar studies have also demonstrated that the $ADC/\Delta ADC$ values have higher diagnostic performances when distinguishing between responders and non-responders, with accuracy rates of 71.4% and 87.5%, respectively [15, 36]. However, our study confirmed that although the ADC value of ESCC increased significantly after NAC, there was no significant difference in pre-/post-NAC ADC and ΔADC values between responders and non-responders' groups. Unlike previous studies, the pathologic response to NAC in our study was relatively similar, without TRG 0 or TRG 1 group as controls, which may affect the diagnostic performances of D and ADC values in predicting the pathological response to NAC. The fact that there were observable differences in the minimal responders does suggest the value of IVIM technique. DWI-derived ADC value is calculated by the mono-exponential diffusion model, which is considered as Brownian diffusion under ideal condition and neglects the influence of microcapillary perfusion [37]. However, diffusion in vivo tissue is more complicated than the Brownian motion. The ADC value is often higher

than the value of true water molecular diffusion and cannot reflect the true tissue diffusion. In this study, the diagnostic performance of the D value is significantly better than the ADC value in evaluating and predicting the pathological response to NAC. Compared with IVIM sequence, traditional DWI technology is stable and simple. Future large sample studies are warranted to assess the predictive value of ADC in assessing response of patient with ESCC to NAC.

Our results also confirmed that the f value of ESCC increased significantly after NAC. A previous study demonstrated a similar trend in f values [26]. This may be related to cellular apoptosis, inflammatory cell infiltration, and expansion of cellular spaces induced by chemotherapy, which may lead to a relative enlargement in microcapillary perfusion and an increase in f value [38]. However, a study on IVIM [33] showed that f value in a human gastric cancer mouse model decreased significantly after treatment, which is inconsistent with our results. Moreover, no significant difference in pre-/post-NAC f and Δf values were found between responders and non-responders' groups, which were inconsistent with the results of the previous study [26]. A possible reason was that f value is more susceptible to measurement and noise variations, which result in poor reproducibility, limiting its clinical value. Therefore, the changes in f values after NT and the utility for evaluating therapeutic response remain controversial [26, 39].

Consistent with previous studies [14, 19, 26, 40], this study also found that the D^* value and related parameters were unreliable in predicting the therapeutic results, probably due to its intrinsic susceptibility to noise and poor measurement reproducibility [39]. Bi-exponential fitting problems, number, and magnitude of b values may be other contributing factors [40]. Although IVIM-DWI is more technically challenging to perform than other modalities, we adopted the iShim technique, intramuscular injection of raceanisodamine hydrochloride, and breathing training to acquire the enough image quality for diagnosis, which can provide a useful reference for future related research.

Our study has several limitations. First, the sample size was relatively small. Second, in this study, we did not compare treatment response on IVIM-DWI to that obtained using other imaging modalities such as FDG-PET/CT or DCE-MRI and

using conventional RECIST criteria. Future studies are necessary to compare the utility of various imaging techniques in assessing treatment response. Third, a total of eleven patients were excluded due to the inferior IVIM image quality before and after NAC. Therefore, the stability of IVIM image quality of esophageal cancer needs to be further improved. Finally, there is no uniform scanning specification for IVIM sequence, and no consensus has been reached on the number and magnitude of b values that ought to be applied in clinical studies [41, 42]. Therefore, further studies are required to optimize image acquisition and post-processing techniques for deriving sufficiently accurate IVIM parameters.

In conclusion, this pilot study demonstrated that IVIM-DWI may be a feasible, non-invasive, and valuable functional imaging technique in predicting pathologic response at advanced ESCC to NAC. The post-NAC D and ΔD values were effective biomarkers for predicting pathologic response to NAC in locally advanced ESCC and ΔD was the most valuable IVIM parameter.

Acknowledgments We thank Prof. Ihab R. Kamel for valuable advices on revised manuscript and language editing.

Funding This study has received funding by the National Natural Science Foundation of China (81972802) and National nature science foundation of Henan Province (182300410355).

Compliance with ethical standards

Guarantor The scientific guarantor of this publication is Jinrong QU, MD, PHD.

Conflict of interest Two of the authors of this manuscript (Shaoyu Wang and Xu Yan) are employees of Siemens. The remaining authors declare no relationships with any companies whose products or services may be related to the subject matter of the article.

Statistics and biometry Yan Zhao, one of the authors has significant statistical expertise.

Informed consent Written informed consent was obtained from all subjects (patients) in this study.

Ethical approval Institutional Review Board approval was obtained.

Methodology

- prospective
- diagnostic or prognostic study
- performed at one institution

References

1. Shapiro J, van Lanschot JJB, Hulshof MCCM et al (2015) Neoadjuvant chemoradiotherapy plus surgery versus surgery alone for oesophageal or junctional cancer (CROSS): long-term results of a randomised controlled trial. *Lancet Oncol* 16(9):1090–1098. [https://doi.org/10.1016/S1470-2045\(15\)00040-6](https://doi.org/10.1016/S1470-2045(15)00040-6)
2. Ando N, Kato H, Igaki H et al (2012) A randomized trial comparing postoperative adjuvant chemotherapy with cisplatin and 5-fluorouracil versus preoperative chemotherapy for localized advanced squamous cell carcinoma of the thoracic esophagus (JCOG9907). *Ann Surg Oncol* 19(1):68–74. <https://doi.org/10.1245/s10434-011-2049-9>
3. Zheng Y, Liu X, Zhang R et al (2018) Neoadjuvant chemotherapy with or without neoadjuvant radiotherapy compared with neoadjuvant chemoradiotherapy for esophageal cancer. *J Thorac Dis* 10(8):4715–4723. <https://doi.org/10.21037/jtd.2018.07.124>
4. Sendler A (2010) Metabolic response evaluation by PET during neoadjuvant treatment for adenocarcinoma of the esophagus and esophagogastric junction. *Recent Results Cancer Res* 182:167–177. https://doi.org/10.1007/978-3-540-70579-6_14
5. Cunningham D, Allum WH, Stenning SP et al (2006) Perioperative chemotherapy versus surgery alone for resectable gastroesophageal cancer. *N Engl J Med* 355(1):11–20. <https://doi.org/10.1056/NEJMoa055531>
6. Griffin Y (2016) Esophageal cancer: role of imaging in primary staging and response assessment post neoadjuvant therapy. *Semin Ultrasound CT MR* 37(4):339–351. <https://doi.org/10.1053/j.sult.2016.02.003>
7. Konieczny A, Meyer P, Schnider A et al (2013) Accuracy of multidetector-row CT for restaging after neoadjuvant treatment in patients with oesophageal cancer. *Eur Radiol* 23(9):2492–2502. <https://doi.org/10.1007/s00330-013-2844-8>
8. Hamai Y, Hihara J, Emi M et al (2016) Ability of fluorine-18 fluorodeoxyglucose positron emission tomography to predict outcomes of neoadjuvant chemoradiotherapy followed by surgical treatment for esophageal squamous cell carcinoma. *Ann Thorac Surg* 102(4):1132–1139. <https://doi.org/10.1016/j.athoracsur.2016.04.011>
9. Joye I, Deroose CM, Vandecaveye V, Haustermans K (2014) The role of diffusion-weighted MRI and (18)F-FDG PET/CT in the prediction of pathologic complete response after radiochemotherapy for rectal cancer: a systematic review. *Radiother Oncol* 113:158–165. <https://doi.org/10.1016/j.radonc.2014.11.026>
10. Lei J, Han Q, Zhu S et al (2015) Assessment of esophageal carcinoma undergoing concurrent chemoradiotherapy with quantitative dynamic contrast-enhanced magnetic resonance imaging. *Oncol Lett* 10(6):3607–3612. <https://doi.org/10.3892/ol.2015.3779>
11. Lu Y, Ma L, Qin J et al (2019) The value of GRASP on DCE-MRI for assessing response to neoadjuvant chemotherapy in patients with esophageal cancer. *BMC Cancer* 19(1):999. <https://doi.org/10.1186/s12885-019-6247-3>
12. Biffar A, Dietrich O, Sourbron S, Duerr HR, Reiser MF, Baur-Melnyk A (2010) Diffusion and perfusion imaging of bone marrow. *Eur J Radiol* 76(3):323–328. <https://doi.org/10.1016/j.ejrad.2010.03.011>
13. Iima M, Le Bihan D (2016) Clinical intravoxel incoherent motion and diffusion MR imaging: past, present, and future. *Radiology* 278(1):13–32. <https://doi.org/10.1148/radiol.2015150244>
14. Li H, Zhang J, Zheng Z et al (2018) Preoperative histogram analysis of intravoxel incoherent motion (IVIM) for predicting microvascular invasion in patients with single hepatocellular carcinoma. *Eur J Radiol* 105:65–71. <https://doi.org/10.1016/j.ejrad.2018.05.032>
15. De Cobelli F, Giganti F, Orsenigo E et al (2013) Apparent diffusion coefficient modifications in assessing gastro-oesophageal cancer response to neoadjuvant treatment: comparison with tumour regression grade at histology. *Eur Radiol* 23(8):2165–2174. <https://doi.org/10.1007/s00330-013-2807-0>
16. Donati F, Boraschi P, Pacciardi F et al (2017) 3T diffusion-weighted MRI in the response assessment of colorectal liver metastases after chemotherapy: correlation between ADC value and

- histological tumour regression grading. *Eur J Radiol* 91:57–65. <https://doi.org/10.1016/j.ejrad.2017.03.020>
17. Le Bihan D, Breton E, Lallemand D, Aubin ML, Vignaud J, Laval-Jeantet M (1988) Separation of diffusion and perfusion in intravoxel incoherent motion MR imaging. *Radiology* 168(2):497–505. <https://doi.org/10.1148/radiology.168.2.3393671>
 18. Le Bihan D (2019) What can we see with IVIM MRI? *Neuroimage* 187:56–67. <https://doi.org/10.1016/j.neuroimage.2017.12.062>
 19. Zhang Y, Kuang S, Shan Q et al (2019) Can IVIM help predict HCC recurrence after hepatectomy? *Eur Radiol* 29(11):5791–5803. <https://doi.org/10.1007/s00330-019-06180-1>
 20. Catanese A, Malacario F, Cirillo L et al (2018) Application of intravoxel incoherent motion (IVIM) magnetic resonance imaging in the evaluation of primitive brain tumours. *Neuroradiol J* 31(1):4–9. <https://doi.org/10.1177/1971400917693025>
 21. Wang LL, Lin J, Liu K et al (2014) Intravoxel incoherent motion diffusion-weighted MR imaging in differentiation of lung cancer from obstructive lung consolidation: comparison and correlation with pharmacokinetic analysis from dynamic contrast-enhanced MR imaging. *Eur Radiol* 24(8):1914–1922. <https://doi.org/10.1007/s00330-014-3176-z>
 22. Baidya Kayal E, Kandasamy D, Khare K, Bakhshi S, Sharma R, Mehndiratta A (2019) Intravoxel incoherent motion (IVIM) for response assessment in patients with osteosarcoma undergoing neoadjuvant chemotherapy. *Eur J Radiol* 119:108635. <https://doi.org/10.1016/j.ejrad.2019.08.004>
 23. Ding Y, Tan Q, Mao W et al (2019) Differentiating between malignant and benign renal tumors: do IVIM and diffusion kurtosis imaging perform better than DWI? *Eur Radiol* 29(12):6930–6939. <https://doi.org/10.1007/s00330-019-06240-6>
 24. Foti PV, Privitera G, Piana S et al (2016) Locally advanced rectal cancer: qualitative and quantitative evaluation of diffusion-weighted MR imaging in the response assessment after neoadjuvant chemo-radiotherapy. *Eur J Radiol Open* 3:145–152. <https://doi.org/10.1016/j.ejro.2016.06.003>
 25. Fujima N, Yoshida D, Sakashita T et al (2017) Prediction of the treatment outcome using intravoxel incoherent motion and diffusional kurtosis imaging in nasal or sinonasal squamous cell carcinoma patients. *Eur Radiol* 27(3):956–965. <https://doi.org/10.1007/s00330-016-4440-1>
 26. Zheng H, Ren W, Pan X et al (2018) Role of intravoxel incoherent motion MRI in early assessment of the response of esophageal squamous cell carcinoma to chemoradiotherapy: a pilot study. *J Magn Reson Imaging* 48(2):349–358. <https://doi.org/10.1002/jmri.25934>
 27. Mandard AM, Dalibard F, Mandard JC et al (1994) Pathologic assessment of tumor regression after preoperative chemoradiotherapy of esophageal carcinoma. Clinicopathologic correlations. *Cancer* 73(11):2680–2686. [https://doi.org/10.1002/1097-0142\(19940601\)73:11<2680::aid-cnrcr2820731105>3.0.co;2-c](https://doi.org/10.1002/1097-0142(19940601)73:11<2680::aid-cnrcr2820731105>3.0.co;2-c)
 28. Koh DM, Collins DJ, Orton MR (2011) Intravoxel incoherent motion in body diffusion-weighted MRI: reality and challenges. *AJR Am J Roentgenol* 196(6):1351–1361. <https://doi.org/10.2214/AJR.10.5515>
 29. Nougaret S, Vargas HA, Lakhman Y et al (2016) Intravoxel incoherent motion-derived histogram metrics for assessment of response after combined chemotherapy and radiation therapy in rectal cancer: initial experience and comparison between single-section and volumetric analyses. *Radiology* 280(2):446–454. <https://doi.org/10.1148/radiol.2016150702>
 30. Ryan R, Gibbons D, Hyland JM et al (2005) Pathological response following long-course neoadjuvant chemoradiotherapy for locally advanced rectal cancer. *Histopathology* 47(2):141–146. <https://doi.org/10.1111/j.1365-2559.2005.02176.x>
 31. Xiang SF, Zhang XQ, Yang SJ et al (2019) Intravoxel incoherent motion magnetic resonance imaging with integrated slice-specific shimming for old myocardial infarction: a pilot study. *Sci Rep* 9(1):19766. <https://doi.org/10.1038/s41598-019-56489-6>
 32. Zhang H, Xue H, Alto S et al (2016) Integrated shimming improves lesion detection in whole-body diffusion-weighted examinations of patients with plasma disorder at 3 T. *Invest Radiol* 51(5):297–305. <https://doi.org/10.1097/RLI.0000000000000238>
 33. Song XL, Kang HK, Jeong GW et al (2016) Intravoxel incoherent motion diffusion-weighted imaging for monitoring chemotherapeutic efficacy in gastric cancer. *World J Gastroenterol* 22(24):5520–5531. <https://doi.org/10.3748/wjg.v22.i24.5520>
 34. Petrillo A, Fusco R, Granata V et al (2018) Assessing response to neo-adjuvant therapy in locally advanced rectal cancer using intravoxel incoherent motion modelling by DWI data and standardized index of shape from DCE-MRI. *Ther Adv Med Oncol* 10:1758835918809875. <https://doi.org/10.1177/1758835918809875>
 35. van Rossum PS, van Lier AL, van Vulpen M et al (2015) Diffusion-weighted magnetic resonance imaging for the prediction of pathologic response to neoadjuvant chemoradiotherapy in esophageal cancer. *Radiother Oncol* 115(2):163–170. <https://doi.org/10.1016/j.radonc.2015.04.027>
 36. Li QW, Qiu B, Wang B et al (2018) Prediction of pathologic responders to neoadjuvant chemoradiotherapy by diffusion-weighted magnetic resonance imaging in locally advanced esophageal squamous cell carcinoma: a prospective study. *Dis Esophagus* 31(2):1–7. <https://doi.org/10.1093/dote/dox121>
 37. Bae JS, Kim SH, Hur BY et al (2019) Prognostic value of MRI in assessing extramural venous invasion in rectal cancer: multi-readers' diagnostic performance. *Eur Radiol* 29(8):4379–4388. <https://doi.org/10.1007/s00330-018-5926-9>
 38. Hauser T, Essig M, Jensen A et al (2013) Characterization and therapy monitoring of head and neck carcinomas using diffusion-imaging-based intravoxel incoherent motion parameters—preliminary results. *Neuroradiology* 55(5):527–536. <https://doi.org/10.1007/s00234-013-1154-9>
 39. Andreou A, Koh DM, Collins DJ et al (2013) Measurement reproducibility of perfusion fraction and pseudodiffusion coefficient derived by intravoxel incoherent motion diffusion-weighted MR imaging in normal liver and metastases. *Eur Radiol* 23(2):428–434. <https://doi.org/10.1007/s00330-012-2604-1>
 40. Jerome NP, Miyazaki K, Collins DJ et al (2017) Repeatability of derived parameters from histograms following non-Gaussian diffusion modelling of diffusion-weighted imaging in a paediatric oncological cohort. *Eur Radiol* 27(1):345–353. <https://doi.org/10.1007/s00330-016-4318-2>
 41. Cohen AD, Schieke MC, Hohenwarter MD, Schmainda KM (2015) The effect of low b-values on the intravoxel incoherent motion derived pseudodiffusion parameter in liver. *Magn Reson Med* 73(1):306–311. <https://doi.org/10.1002/mrm.25109>
 42. Perucho JAU, Chang HCC, Vardhanabhati V et al (2020) B-value optimization in the estimation of intravoxel incoherent motion parameters in patients with cervical cancer. *Korean J Radiol* 21(2):218–227. <https://doi.org/10.3348/kjr.2019.0232>

Publisher's note Springer Nature remains neutral with regard to jurisdictional claims in published maps and institutional affiliations.